

# *Characterization of cutaneous and articular sensory neurons*

Article

Published Version

Creative Commons: Attribution-Noncommercial 3.0

Open Access

da Silva Serra, I., Husson, Z., Bartlett, J. D. and Smith, E. S. J. (2016) Characterization of cutaneous and articular sensory neurons. *Molecular Pain*, 12. 1744806916636387. ISSN 1744-8069 doi: 10.1177/1744806916636387 Available at <https://centaur.reading.ac.uk/65958/>

It is advisable to refer to the publisher's version if you intend to cite from the work. See [Guidance on citing](#).

Published version at: <http://dx.doi.org/10.1177/1744806916636387>

To link to this article DOI: <http://dx.doi.org/10.1177/1744806916636387>

Publisher: Sage

All outputs in CentAUR are protected by Intellectual Property Rights law, including copyright law. Copyright and IPR is retained by the creators or other copyright holders. Terms and conditions for use of this material are defined in the [End User Agreement](#).

[www.reading.ac.uk/centaur](http://www.reading.ac.uk/centaur)

**CentAUR**

Central Archive at the University of Reading

Reading's research outputs online

# Characterization of cutaneous and articular sensory neurons

Ines da Silva Serra, MPharm<sup>1,2,\*</sup>, Zoé Husson, MSc, PhD<sup>1,\*</sup>, Jonathan D. Bartlett<sup>1</sup> and Ewan St. John Smith, MPharmacol, PhD<sup>1</sup>

## Abstract

**Background:** A wide range of stimuli can activate sensory neurons and neurons innervating specific tissues often have distinct properties. Here, we used retrograde tracing to identify sensory neurons innervating the hind paw skin (cutaneous) and ankle/knee joints (articular), and combined immunohistochemistry and electrophysiology analysis to determine the neurochemical phenotype of cutaneous and articular neurons, as well as their electrical and chemical excitability.

**Results:** Immunohistochemistry analysis using RetroBeads as a retrograde tracer confirmed previous data that cutaneous and articular neurons are a mixture of myelinated and unmyelinated neurons, and the majority of both populations are peptidergic. In whole-cell patch-clamp recordings from cultured dorsal root ganglion neurons, voltage-gated inward currents and action potential parameters were largely similar between articular and cutaneous neurons, although cutaneous neuron action potentials had a longer half-peak duration (HPD). An assessment of chemical sensitivity showed that all neurons responded to a pH 5.0 solution, but that acid-sensing ion channel (ASIC) currents, determined by inhibition with the nonselective acid-sensing ion channel antagonist benzamil, were of a greater magnitude in cutaneous compared to articular neurons. Forty to fifty percent of cutaneous and articular neurons responded to capsaicin, cinnamaldehyde, and menthol, indicating similar expression levels of transient receptor potential vanilloid 1 (TRPV1), transient receptor potential ankyrin 1 (TRPA1), and transient receptor potential melastatin 8 (TRPM8), respectively. By contrast, significantly more articular neurons responded to ATP than cutaneous neurons.

**Conclusion:** This work makes a detailed characterization of cutaneous and articular sensory neurons and highlights the importance of making recordings from identified neuronal populations: sensory neurons innervating different tissues have subtly different properties, possibly reflecting different functions.

## Keywords

Acid-sensing ion channel, ion channel, skin, joint, dorsal root ganglia, nociception, pain

Date received: 26 January 2016; accepted: 2 February 2016

## Background

Throughout the animalia kingdom, organisms possess sensory neurons that enable them to detect their external and internal environments, some of which are dedicated to the transduction of solely noxious stimuli, so-called nociceptors.<sup>1–5</sup> The majority of cell bodies of sensory neurons are located in the dorsal root ganglia (DRG, which innervate the body) and trigeminal ganglia (which innervate the head), and neuronal culture of these ganglia is a widely used technique to investigate sensory neuron function.<sup>6</sup>

The DRG are often taken either from the entire animal or from a relevant anatomical location, for example, in studies where the sciatic nerve has been injured, lumbar DRG are often used. However, DRG neurons

are not a uniform population and different subtypes have been described based on their electrophysiological properties and immunochemical profiles. Single-cell RNA sequencing analysis of mouse lumbar DRG neurons has recently demonstrated that these neurons can be

<sup>1</sup>Department of Pharmacology, University of Cambridge, Cambridge, UK

<sup>2</sup>School of Psychology and Clinical Language Sciences, University of Reading, Reading, UK

\*These authors contributed equally.

### Corresponding author:

Ewan St. John Smith, Department of Pharmacology, University of Cambridge, Tennis Court Road, Cambridge, CB2 1PD, UK.  
Email: es336@cam.ac.uk



split into 11 different populations based upon RNA expression,<sup>7</sup> and functional analysis conducted by a variety of research groups has also demonstrated that isolated mouse and rat DRG neurons can be split into different groups depending upon their electrical, thermal, and chemical sensitivity.<sup>8–12</sup> In vitro differences are observed between peptidergic and nonpeptidergic neurons, distinguished by their isolectin B4 (IB4) binding, an in vitro marker of nonpeptidergic neurons.<sup>13</sup> For example, acid evokes transient, rapidly inactivating inward currents that are mediated by acid-sensing ion channels (ASICs) more frequently in IB4-negative neurons than in IB4-positive neurons,<sup>8–10,14</sup> and IB4-positive neurons have longer action potential durations than IB4-negative neurons.<sup>11,12</sup>

To identify the nature and characterize the properties of neurons innervating specific sites, it is necessary to specifically label the different neuronal populations within the DRG. Retrograde tracing involves injecting a small volume of fluorescent tracer at the site of interest (e.g. skin/joints), allowing, after a few days, DRG to be cultured and imaging methods used to identify labeled neurons. Using this technique, we have previously identified that transient receptor potential vanilloid 4 (TRPV4) makes a significant contribution to the osmosensitivity of mouse hepatic afferent neurons,<sup>15</sup> others have demonstrated that ASIC3 produces acid sensitivity in rat cardiac afferents<sup>16</sup> and is the major contributor to the acid sensitivity of rat dorsal paw skin afferents,<sup>17</sup> and other research groups have determined the properties of sensory neurons innervating a wide range of tissues.<sup>18–22</sup>

Previous studies using retrograde tracing in mice and rats showed that neurons innervating joints and skin have different neurochemical profiles. Approximately, 50% of ankle/knee joint afferents are positive for calcitonin gene-related peptide (CGRP, a marker of peptidergic neurons, expressed by both myelinated and unmyelinated neurons) while knee afferent neurons have either been found to be IB4-negative<sup>23–25</sup> or to display very low (1.5%) levels of IB4 binding.<sup>26</sup> In contrast, neurons innervating the skin in various sites of the body are more frequently IB4-positive, although to varying degrees,<sup>27–29</sup> and one study found that approximately 20% of plantar skin afferents are IB4-positive.<sup>30</sup> Additionally, the receptor for nerve growth factor, TrkA, which is expressed by peptidergic neurons, is expressed by approximately 40% of rat neurons innervating the footpad.<sup>31</sup> However, in none of these studies was electrophysiology conducted to further characterize functional properties of identified neurons. For example, electrophysiological analysis of action potential waveform can be used to determine the likelihood that a neuron is a nociceptor or a mechanoreceptor: nociceptors have longer action potential durations, often characterized by an inflection, or hump, on their falling phase,<sup>32</sup> even in an isolated preparation.

In this study, we retrogradely labeled cutaneous (hind paw plantar skin) and articular (ankle and knee joints) sensory neurons and combined immunohistochemistry and whole-cell patch clamp recordings to characterize their comparative neurochemical phenotypes and their relative electrical and chemical excitabilities. We found that both cutaneous and articular neurons are mostly peptidergic and that cutaneous neurons have larger ASIC-mediated currents, whereas articular neurons are more likely to respond to ATP.

## Methods

### Animals

All experiments were conducted in accordance with the United Kingdom Animal (Scientific Procedures) Act 1986 under a Project License (70/7705) granted to E. St. J. S. by the Home Office; the University of Cambridge Animal Welfare Ethical Review Body also approved procedures. Female C57/bl6 mice (four to six weeks) were used in this study because rheumatoid arthritis is more prevalent in females and thus they are our focus and were bred in house. Mice were conventionally housed in groups of up to five mice per cage with nesting material and a red plastic shelter; the holding room was temperature controlled (21°C) and mice were on a normal 12-h light/dark cycle with food and water available ad libitum. Technicians observed mice daily and a study plan outlining the procedures, with a description of possible adverse effects, was kept in the room where mice were housed.

### Retrograde tracer injections

In a designated procedure room, animals were weighed and anaesthetized using ketamine (100 mg/kg) and xylazine (10 mg/kg); injectable anesthesia was used because it allows subsequent manipulation of mice to enable administration of retrograde tracer. Lumafluor rhodamine-labeled latex spheres (0.02–2 µm), RetroBeads,<sup>33</sup> were diluted 1:2.5 in MilliQ water. Once no withdrawal reflexes were observed, mice received retrograde tracer subcutaneous injections to the lateral (~1 µl), central (~1 µl), and medial (~1 µl) plantar aspects of both hind paws to label cutaneous afferents across the plantar surface of the hind paws. Alternatively, to label articular afferent neurons, retrograde tracer injections were administered to both hind limb knees (~1.5 µl) and ankles (~2.5 µl). Injections were performed using a 10 µl Hamilton syringe and a 30 G needle. Mice were housed in a recovery chamber (30°C) and observed by a theatre technician until fully alert, at which point they were returned to the holding room. For immunohistochemistry experiments, four mice were used for the

cutaneous group and four mice for the articular group. For electrophysiology experiments, 5 mice were used for the cutaneous group and 10 mice for the articular group; more mice were needed for the articular group because of the relative paucity of labeled neurons observed in culture. In accordance with the 3Rs, brains were removed from mice for use in other experiments to reduce the total number of animals used.

### DRG dissection and culture

Mice were killed four to six days after retrograde tracer injection by cervical dislocation and lumbar (L2–L5) DRG were removed and collected in  $\text{Ca}^{2+}$ – $\text{Mg}^{2+}$ –free phosphate-buffered saline (PBS); skin, or knees and ankles were always dissected to ensure that appropriate administration of retrograde tracer had been performed. DRG were subsequently incubated in collagenase IV (500  $\mu\text{g}/\text{ml}$ , 30 min, 37°C, Sigma-Aldrich, C5138, St. Louis, MO) in DRG culture medium (Dulbecco's Modified Eagle Medium; Life Technologies, 21331-020, Carlsbad, CA) containing 10% heat-inactivated horse serum (Life Technologies, 26050-088), 2 mM glutamine, 0.4% glucose, 100U penicillin, and 100 mg/ml streptomycin (Life Technologies), followed by incubation in trypsin (0.0125%, 25 min, 37°C, Sigma T4174). DRGs were washed twice with DRG culture medium and then triturated using 20G ( $\times 5$ ) and 23G ( $\times 2$ –3) needles. Dissociated neurons were plated on to poly-D-lysine-coated MatTek glass bottom dishes (P35GC-1.5-14-C), which had been coated with laminin (20  $\mu\text{g}/\text{ml}$ , 2 hr at 37°C before washing twice with water, Life Technologies 23017015). Neurons were kept at 37°C in 5%  $\text{CO}_2$ .

### Immunohistochemistry

Mice were killed four days following retrograde tracer injection by cervical dislocation and lumbar (L2–L5) DRG were removed and collected in 4% paraformaldehyde (PFA) on ice. After 30-min incubation, DRG were placed in 30% sucrose overnight at 4°C for cryoprotection. DRG were subsequently embedded in optimum cutting temperature (OCT) compound and stored at  $-20^\circ\text{C}$ . DRG sections (12  $\mu\text{m}$ ) were cut using a Leica Cryostat CM3000, mounted on to Superfrost Plus microscope slides (Thermo Scientific), and stored at  $-20^\circ\text{C}$  until processed.

Sections were blocked with a pre-incubation buffer of 1% bovine serum albumin (BSA; Sigma, A7906) for 2 h at room temperature, except for the slides for use with anti-peripherin antibody, which were blocked with a 2% BSA and 10% goat serum (Life Technologies, 10658654) buffer and the ones for use with the anti-CGRP antibody which were blocked with a 2% BSA and 4% donkey

serum (Sigma, D9663) buffer. Sections were subsequently incubated overnight, with primary antibodies at 4°C: goat anti-transient receptor potential vanilloid 1 (TRPV1; Santa Cruz Biotechnology sc-12498, 1:1000) in a 1% BSA and 0.1% fish gelatin (Sigma, G7041) buffer; rabbit anti-NF-200 (Sigma N4142, 1:1000) in a 5% goat serum buffer; chicken anti-peripherin (Abcam ab39374, 1:500) in a 2% BSA and 4% goat serum buffer; rabbit anti-CGRP (Sigma C8198, 1:10,000) in a 2% BSA and 4% donkey serum buffer. After three rinses of the antibody slides in tris-buffered saline (TBS), sections were incubated with appropriate Alexa 488-conjugated secondary antibodies (goat anti-chicken, Abcam ab150169; donkey anti-goat, Life Technologies A11055; and goat anti-rabbit, Life Technologies A11008; all used at 1:1000) for 2 hrs at room temperature and finally rinsed three times in TBS, once with MilliQ water, and mounted using FluorSave (Merck). For IB4-Alexa-488 (IB4, Life Technologies, 4  $\mu\text{g}/\text{ml}$ ) staining, slides were incubated in the electrophysiology extracellular solution (see below) for 20 min at room temperature, rinsed three times with TBS, once with MilliQ water, and then mounted using FluorSave.

Sections were analyzed using a Zeiss Aksioskop microscope; nonconsecutive sections were analyzed to prevent counting the same cell twice, and the same number of sections was counted from each animal. Pictures were taken for each section both for the bright field and fluorescent channels as appropriate for the antibody and Lumafluor beads, using a 40 $\times$  objective. The exposure time used for each particular antibody was the same for each section so that the quality of staining was comparable between sections.

Sections were analyzed using ImageJ software. Each neuron was detected on the bright field image and defined as a region of interest (ROI) by manual drawing of its perimeter. ROI statistics (notably the mean intensity) were then retrieved for each ROI on individual fluorescent channel pictures (for RetroBeads and antibodies). For determination of the CGRP, peripherin, NF-200, and TRPV1 immunoreactivity, a custom routine using GNU R was used. For each section, the mean intensity distribution was plotted revealing a bimodal distribution. The peak at low intensities values represented the population of negative cells and could be approximated by a Gaussian function. A long tail at higher intensity values represented the strongly labeled cells, which were considered positive when their mean intensity value was above a cut-off value defined as two times the standard deviation above the mean intensity value of the population of negative cells. Due to the membrane labeling of cells by IB4, it was not possible to use the cell intensity method described earlier; instead, labeling was determined manually by two independent experimenters. For all markers, a cell was considered



as labeled by Lumafluor RetroBeads if five or more beads were present within its cell body.

Data were analyzed and plotted using Excel (Microsoft) and Prism (GraphPad). A one-way analysis of variance (ANOVA) and Tukey's post hoc test were used to analyze differences in the percentage of RetroBeads in different lumbar DRG following cutaneous or articular injection; the unit of analysis was the number of images analyzed for each ganglia and two to five images were analyzed per lumbar level per mouse. A one-way ANOVA and Tukey's post hoc test were used to analyze differences in the frequency of colocalization of RetroBeads with each marker used following cutaneous or articular injection; the unit of analysis was the number of mice per condition ( $n=4$  per condition).

### Electrophysiology

DRG neuron recordings were made on the day after dissection (24–32 h post-dissection), using the following solutions: extracellular (in mM)—NaCl (140), KCl (4),  $\text{CaCl}_2$  (2),  $\text{MgCl}_2$  (1), glucose (4), HEPES (10), adjusted to pH 7.4 with NaOH; intracellular (in mM)—KCl (110), NaCl (10),  $\text{MgCl}_2$  (1), EGTA (1), and HEPES (10), adjusted to pH 7.3 with KOH. Acidic extracellular solutions were made using MES (pH 5.0). Prior to beginning recordings, neurons were incubated in IB4-Alexa-488 (2  $\mu\text{g}/\text{ml}$ ) for 15 min; cells were then washed with extracellular solution for 10 min. We only made recordings from neurons in which 5+ RetroBeads could be observed and only neurons in which an action potential could be generated and that had a resting membrane potential of  $-40\text{ mV}$  or more negative were used for experiments. Patch pipettes were pulled (P-97, Sutter Instruments) from borosilicate glass capillaries (Hilgenberg) and had a resistance of 3–6 M $\Omega$ . Recordings were made using an EPC-10 amplifier (HEKA) and Patchmaster© software (HEKA). Whole-cell currents were recorded at 20 kHz, pipette and membrane capacitance was compensated using Patchmaster macros, and series resistance was compensated by >60%. In DRG neurons, a standard voltage-step protocol was used, whereby cells were held at  $-120\text{ mV}$  for 240 ms before stepping to the test potential ( $-50\text{ mV}$  to  $+50\text{ mV}$  in 5 mV increments) for 40 ms, returning to the holding potential ( $-60\text{ mV}$ ) for 200 ms between sweeps; leak subtraction was used to minimize capacitive currents. To generate action potentials, we used repetitive 80 ms current injections from 10 pA to 150 pA in 10 pA steps (100–1000 pA in 50 pA steps for larger cells) and the first action potential evoked was analyzed; a hump on the repolarization phase, determined by plotting  $dV/dt$ , was used to classify a cell as a nociceptor. Subsequently, cells were exposed to a 5-s pulse of pH 5.0, 50  $\mu\text{M}$  ATP (Sigma

A26209), 1  $\mu\text{M}$  capsaicin (Sigma, 21750), 100  $\mu\text{M}$  cinnamaldehyde (Merck, 802505), 100  $\mu\text{M}$  menthol (Alfa Aesar A1047418), applied in a random order with a 30-s wash time in between different stimuli; random order of stimulation was conducted to preclude any potential stimulus-mediated sensitization biasing results. Responses to acidic solutions were classified as transient or sustained based upon the initial response, e.g. a rapidly inactivating transient current, followed by a sustained current during the acid application, was classified as a transient response. To determine the contribution of ASICs to transient acid-mediated responses, the nonselective ASIC antagonist benzamil (250  $\mu\text{M}$ , Santa Cruz sc-201070) was applied for 60 s before measuring the response to the pH 5.0 solution again; a 60-s wash period then took place, followed by a final 5-s pH 5.0 stimulation. Images of neurons using a 40 $\times$  objective were captured using a Zyla 5.5 sCMOS camera (Andor), followed by subsequent analysis in ImageJ, having used a stage micrometer to convert pixel values into  $\mu\text{m}$ .

Current amplitude was measured in Fitmaster (HEKA) by taking the maximum peak response and subtracting the mean baseline amplitude in the preceding 10 ms (voltage-gated currents) or  $\sim 2.5\text{ s}$  (chemosensitive currents); current amplitude was normalized for cell size by dividing by cell capacitance. Action potential parameters (amplitude, half-peak duration [HPD], and after-hyperpolarization duration [AHP]) were measured in Igor Pro using in house macros. Data are expressed as mean  $\pm$  standard error of the mean (SEM). Paired  $t$  tests were used to compare the effects of antagonists on proton-gated currents within both cutaneous and articular neuron data sets; unpaired  $t$  tests were used to compare parameters, such as resting membrane potential and transient acid-gated current amplitude, between cutaneous and articular neuron data sets. Fisher's exact test was used to compare the frequency of response to different agonists between cutaneous and articular neurons.

## Results

### Retrograde tracing of articular and cutaneous afferents

Initial control experiments demonstrated that following injection of RetroBeads to either cutaneous or articular regions, no RetroBeads were observed in thoracic ganglia (data not shown), i.e. as others have found,<sup>33</sup> RetroBeads do not diffuse far from the injection site. Similarly, when only the left or right hind limb was used for injection, no RetroBeads were found in lumbar DRG from the contralateral side (data not shown).

Following articular RetroBead injection, the L2 and L5 DRG had the smallest number of labeled neurons ( $0.58 \pm 0.26\%$ , and  $0.58 \pm 0.18\%$ , respectively,

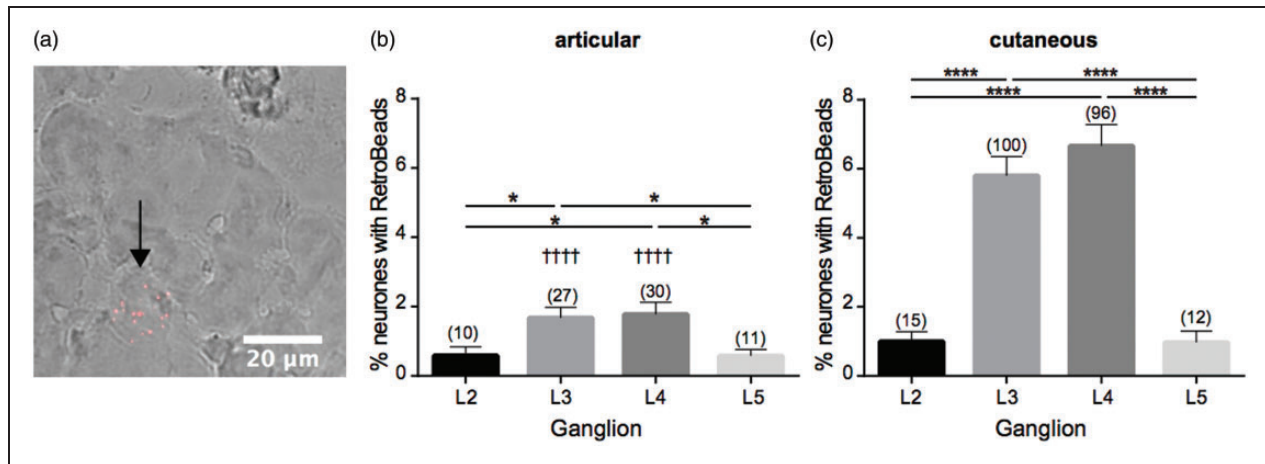


**Figure 1.** Retrograde labeling of articular and cutaneous neurons. (a) DRG section, black arrow indicates neuron containing multiple RetroBeads. Quantification of percentage of neurons containing RetroBeads in L2–L5 DRG following injection of retrograde tracer to articular (b) or cutaneous (c) sites. Numbers in brackets refer to number of retrogradely labeled neurons counted per conditions. \* $p < 0.05$  and \*\*\*\* $p < 0.0001$  between DRG in one set of animals; ††† $p < 0.0001$  between DRG of articular compared with cutaneous animals (one-way ANOVA and Tukey's post hoc test). DRG: dorsal root ganglia; ANOVA: analysis of variance.

Figure 1(a) and (b)) and the L4 DRG contained the highest percentage ( $1.78 \pm 0.35\%$ , Figure 1(b)), a finding which replicates that of others.<sup>24</sup> Following cutaneous RetroBead injection, the L3 and L4 DRG were again found to contain the highest percentage of labeled neurons with the L4 DRG containing the highest percentage ( $6.66 \pm 0.62\%$ , Figure 1(c)), an observation similar to what others have found.<sup>34</sup> In general, more DRG neurons were labeled following cutaneous injection than following articular injection and when comparing the L3 and L4 DRG, the increase was significant ( $p < 0.0001$ , Figure 1(b)).

### Neurochemical phenotype of articular and cutaneous afferents

We next investigated whether primary afferent neurons that innervate the ankles and knees have a similar neurochemical phenotype to cutaneous primary afferent neurons. To ensure that the mice used for articular analysis were neurochemically similar to those used for cutaneous analysis, we first analyzed L2–L5 DRG neurons in the two sets of mice to determine the total percentage of myelinated (NF-200 positive), unmyelinated (peripherin positive), nonpeptidergic (IB4-positive), peptidergic (CGRP positive) and TRPV1-expressing (TRPV1-positive) neurons; it should, however, be noted that NF-200 staining can occur in unmyelinated neurons.<sup>35</sup> As expected, the percentage of neurons positive for each of these markers was not significantly different between the two groups (data not shown). We next determined the neurochemical profiles of articular and cutaneous neurons (example micrographs are shown in

Figure 2(a)–(d)) by assessing colocalization between RetroBead-labeled neurons and different markers. A significantly greater proportion of labeled articular neurons were peptidergic (CGRP positive) compared to nonpeptidergic (IB4-positive;  $79.38 \pm 10.63\%$  and  $5.00 \pm 5.00\%$ , respectively,  $p < 0.01$ , Figure 2(e)). Similarly, articular neurons were predominantly myelinated (NF-200 positive,  $86.67 \pm 8.16\%$ ) compared to nonpeptidergic (IB4-positive) and TRPV1-positive neurons ( $20.83 \pm 10.49\%$ ,  $p < 0.01$ , Figure 2(e)). However, there was no significant difference between the proportion of myelinated (NF-200 positive) and unmyelinated (peripherin positive,  $45.83 \pm 18.48\%$ ) articular neurons. A similar pattern was observed for cutaneous neurons where significantly more labeled neurons were peptidergic (CGRP positive) than nonpeptidergic (IB4-positive;  $84.88 \pm 2.83\%$  and  $26.01 \pm 10.11\%$ , respectively,  $p < 0.05$ , Figure 2(f)). Like articular neurons, there was no significant difference between the myelinated and unmyelinated populations (NF-200 and peripherin positive,  $58.33 \pm 10.41\%$  and  $38.18 \pm 16.63\%$ , respectively; Figure 2(f)). Overall, no significant differences in the neurochemical profiles of articular and cutaneous neurons were found.

### Electrical excitability of articular and cutaneous afferents

Articular and cutaneous afferents were identified in culture by the presence of RetroBeads in the cell cytoplasm and were further classified as being IB4-positive or IB4-negative (Figure 3(a)). Of identified articular and cutaneous neurons, 2/16 and 4/20 were IB4-positive, respectively; because of the small number of IB4-positive

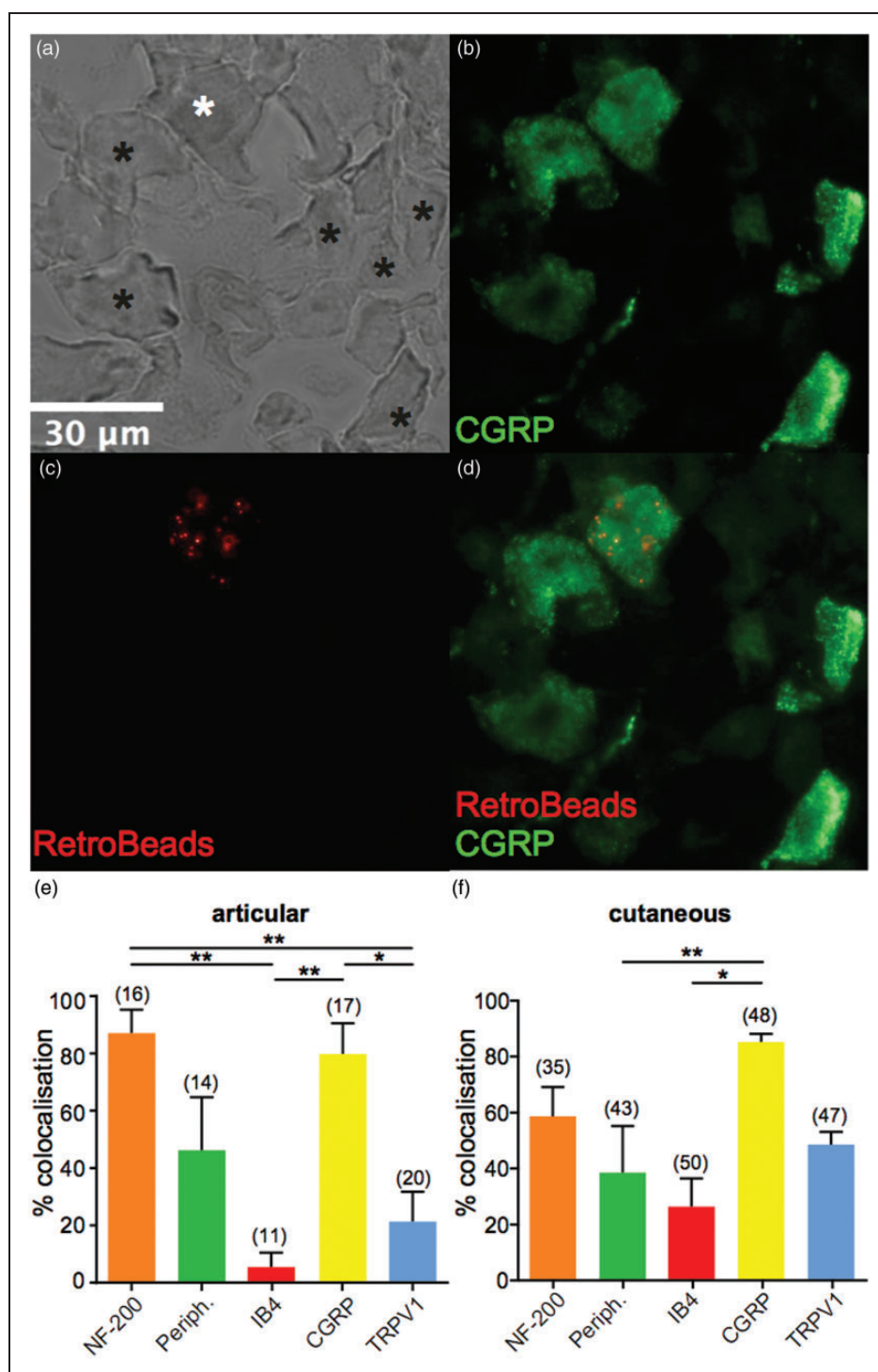


**Figure 2.** Neurochemical phenotype of lumbar DRG and characterization of articular and cutaneous neuron neurochemical composition. (a–d), example micrographs showing a bright field image of a lumbar DRG section (a), white asterisk shows a neuron that is peptidergic (CGRP positive) (b) and contains RetroBeads (c), black asterisks denotes neurons that are CGRP positive but do not contain RetroBeads, and (d) shows the merged image. (e and f) Percentage of lumbar DRG neurons (combined analysis of L2–L5) that colocalize RetroBeads with different neurochemical markers following injection of retrograde tracer to articular (e) or cutaneous (f) sites ( $n = 4$  animals in each condition). Numbers in brackets refer to the number of RetroBeads labeled neurons upon which this analysis is based. \* $p < 0.05$ , \*\* $p < 0.01$  (one-way ANOVA and Tukey's post hoc test). DRG: dorsal root ganglia; CGRP: calcitonin gene-related peptide; ANOVA: analysis of variance.



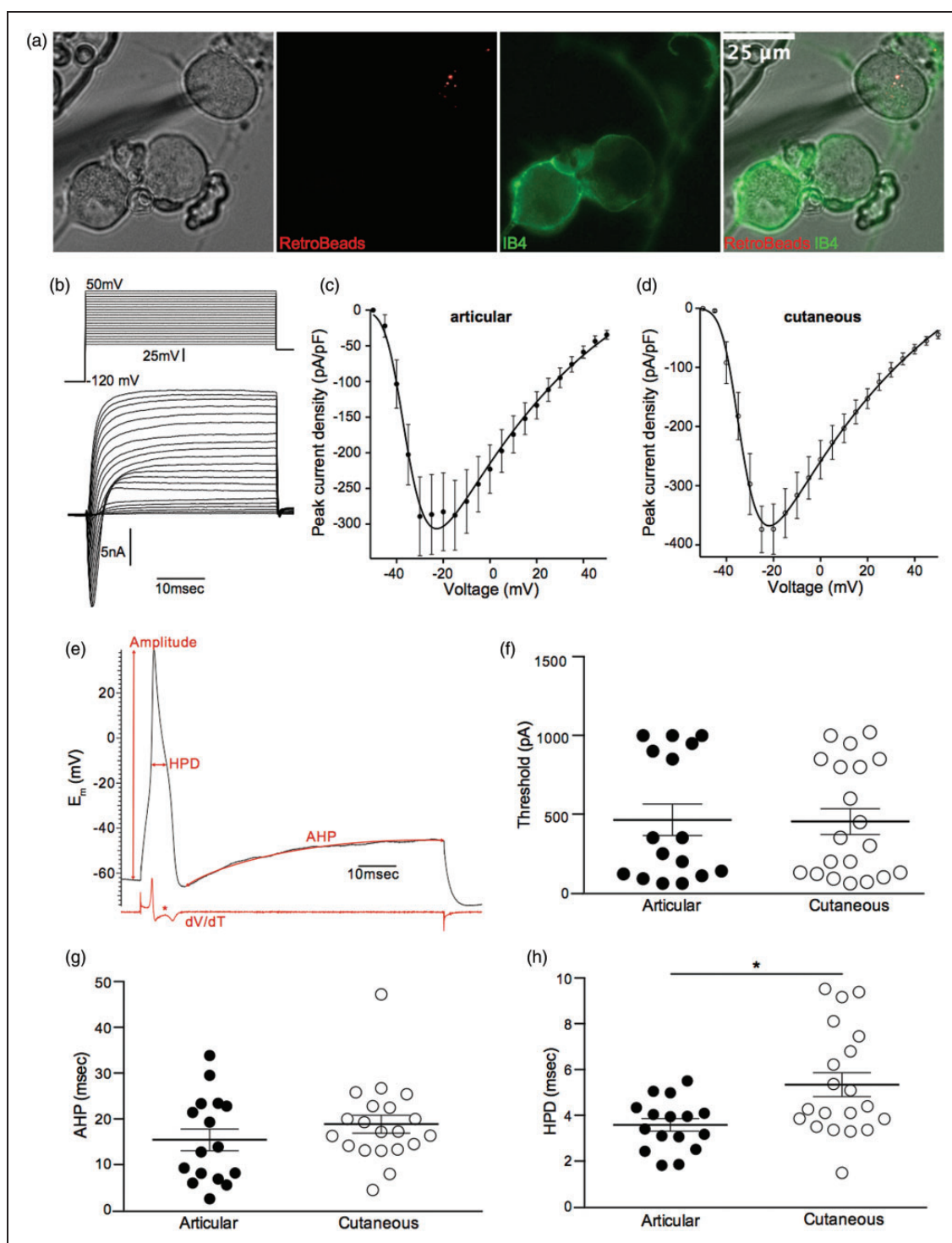


**Figure 3.** Electrical excitability of articular and cutaneous neurons. (a) Images of an articular neuron containing RetroBeads that is IB4-negative. (b) Lower panel, example trace of voltage-gated currents evoked by the voltage-step protocol in the upper panel (see Electrophysiology Section for more details). (c and d) IV curves for voltage-gated inward currents recorded in articular ( $n = 14$ ) and cutaneous ( $n = 18$ ) neurons, respectively. (e) Example action potential evoked by current injection of 350 pA in a cutaneous neuron, red arrows indicate how measurements of amplitude, HPD, and AHP were made; the red trace below the action potential shows a plot of  $dV/dT$ , the asterisk denoting the prominent hump during repolarization. (f-h) action potential parameters: (f) action potential threshold; (g) action potential AHP and (h) action potential HPD recorded in articular ( $n = 14$ ) and cutaneous ( $n = 18$ ) neurons. \* $p < 0.05$ . IB4: isolectin B4; AHP: afterhyperpolarization duration; IV: current voltage relationship; HPD: half peak duration.

**Table 1.** Properties of articular and cutaneous neurons.

	Diameter ( $\mu\text{m}$ )	Resting membrane potential (mV)	AP threshold (pA)	AP HPD (ms)	AP AHP (ms)	AP amplitude (mV)
Articular ( $n = 16$ )	$25.42 \pm 1.34$	$-49.88 \pm 1.86$	$464.40 \pm 99.87$	$3.58 \pm 0.28$	$15.44 \pm 2.37$	$35.26 \pm 3.24$
Cutaneous ( $n = 20$ )	$25.02 \pm 1.08$	$-50.10 \pm 1.08$	$453.50 \pm 80.86$	$5.34 \pm 0.52^{**}$	$18.88 \pm 1.97$	$45.37 \pm 2.50^*$

AP: action potential; HPD: half-peak duration; AHP: afterhyperpolarization duration.

neurons, no further analysis was made of IB4-positive versus IB4-negative neurons. Of the neurons recorded, there was no significant difference in average diameter or resting membrane potentials between articular and cutaneous neurons (Table 1).

To investigate the contribution of voltage-gated  $\text{Na}^+$  currents to macroscopic voltage-gated inward currents, we used a voltage-step protocol previously established for this purpose.<sup>36</sup> We observed that peak voltage-gated inward currents in cutaneous neurons were similar to those in articular neurons (Figures 3(b)–(d) and Table 1). Using current injection to evoke action potentials, there was no significant difference in either the threshold for action potential generation (articular:  $464.40 \pm 99.87$  pA,  $n = 16$  and cutaneous:  $453.50 \pm 80.86$  pA,  $n = 20$ , Figure 3(f)) or the AHP (articular:  $15.44 \pm 2.37$  ms,  $n = 16$  and cutaneous:  $18.88 \pm 1.97$  ms,  $n = 20$ , Figure 3(g)), but the HPD of articular neuron action potentials was significantly shorter than that of cutaneous neurons (articular:  $3.58 \pm 0.28$  ms,  $n = 16$  and cutaneous:  $5.34 \pm 0.52$  ms,  $n = 20$ ,  $p < 0.01$ , Figure 3(h)). All of the neurons recorded from had an inflection, or hump, on the falling phase (Figure 3(e)), which indicates that they were all putative nociceptors.<sup>32</sup>

### pH sensitivity of articular and cutaneous afferents

To determine the nature of acid-gated currents and putative differences between articular and cutaneous afferent neurons, neurons were exposed to a 5-s pulse of a pH 5.0 solution. If a transient current was recorded, the ASIC antagonist benzamil (250  $\mu\text{M}$ ) was applied for 60 s before reapplying a pH 5.0 solution. In both articular and cutaneous neurons, the majority of acid-gated currents were rapidly inactivating transient currents, where inactivation to baseline never fully occurred leaving a small sustained current recorded throughout the period stimulation (articular: 10/16 neurons and cutaneous: 15/20 neurons, Figure 4(a)). Moreover, the peak transient phase (T) of these rapidly inactivating currents was sensitive to benzamil inhibition, but the smaller sustained phase (Ts) was not (articular: T control  $15.72 \pm 3.68$  pA/pF, T benzamil  $2.70 \pm 0.92$  pA/pF,  $n = 10$ ,  $p < 0.01$ , Figure 4(b); cutaneous: T control  $34.05 \pm 6.44$  pA/pF, T benzamil  $6.29 \pm 1.51$  pA/pF,  $n = 15$ ,  $p < 0.001$ , Figure 4(c)), thus indicating that the peak transient

acid-gated currents were mediated by ASICs, whereas the sustained acid-gated current may involve non-ASIC conductances, although the inability of benzamil and its derivatives to fully inhibit the sustained phase of ASIC-mediated currents has been previously documented.<sup>36,37</sup> Comparing the magnitude of the ASIC-like currents between articular and cutaneous neurons, cutaneous neuron currents were significantly larger ( $34.05 \pm 6.44$  pA/pF,  $n = 15$  vs.  $15.72 \pm 3.68$  pA/pF,  $n = 10$ ,  $p < 0.05$ , Figure 4(b) and (c)). However, no significant difference was observed in the inactivation time constant of these transient currents (articular:  $144.0 \pm 15.58$  ms,  $n = 9$  and cutaneous:  $151.1 \pm 15.49$  ms,  $n = 13$ ), suggesting that the nature of ASIC subunits responsible for the transient currents observed is similar between articular and cutaneous neurons. Of the sustained currents recorded, sensitivity to capsaicin was demonstrated in approximately half the cases (articular: 3/6 neurons and cutaneous: 2/5 neurons, Figure 4(d) and (e)).

### Chemosensitivity of articular and cutaneous afferents

To investigate the chemosensitivity of articular and cutaneous afferent neurons, neurons were exposed to 5-s pulses of capsaicin (1  $\mu\text{M}$ , TRPV1 agonist), cinnamaldehyde (100  $\mu\text{M}$ , transient receptor potential ankyrin 1 [TRPA1] agonist), menthol (100  $\mu\text{M}$ , transient receptor potential melastatin 8 [TRPM8] agonist), and ATP (50  $\mu\text{M}$ , P2X/P2Y agonist). The percentage of articular and cutaneous neurons responding to the transient receptor potential (TRP) channel agonists was highly similar (Figure 5(a)–(c)), but a significantly smaller proportion of cutaneous neurons displayed a response to ATP (Figure 5(d), articular: 87.5% responders and cutaneous: 50.0% responders,  $p < 0.05$ ). Of the articular/cutaneous neurons that responded to ATP, currents were either transient P2X-like responses or sustained P2Y-like responses (Figure 5(e)) and similar proportions of responses to ATP were P2Y-like in both articular and cutaneous neurons (Figure 5(f)).

By comparing the peak current densities for responses to capsaicin, cinnamaldehyde, menthol, and ATP, we observed no significant differences in the amplitude of responses between articular and cutaneous neurons (Figure 5(g)). Similarly, comparison of the P2X-like and P2Y-like currents showed that there was no

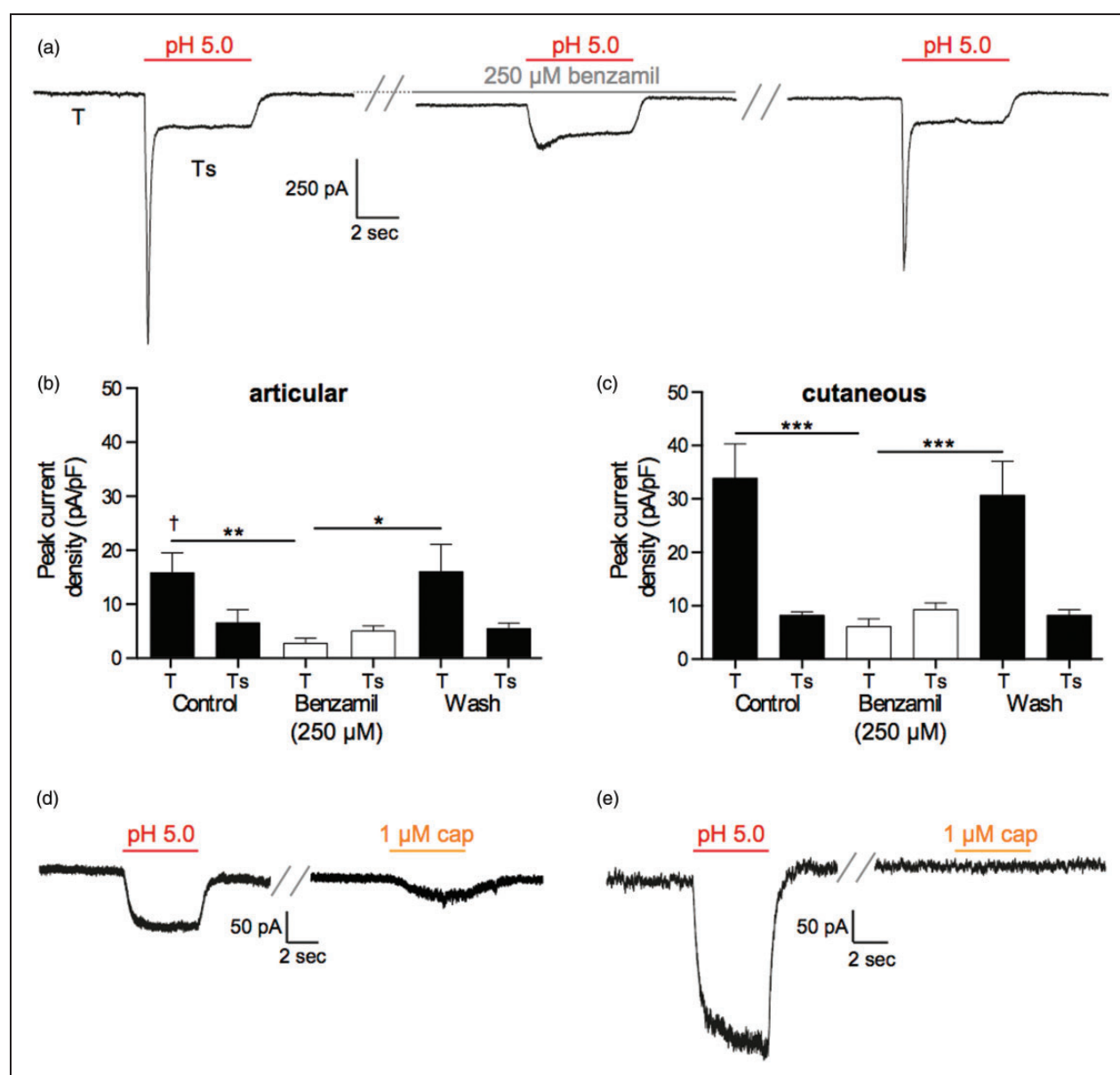


**Figure 4.** pH sensitivity of articular and cutaneous neurons. (a) Example of a transient current evoked by a 5-s application of a pH 5.0 solution (left panel: T labels the peak transient current and Ts labels the sustained phase) that is inhibited by 60 s of benzamil (250  $\mu$ M) treatment (middle panel) and recovers following a 60-s wash (right panel). (b and c), benzamil inhibition of the T, but not the Ts, phase of rapidly inactivating currents in articular ( $n = 10$ ) and cutaneous ( $n = 15$ ) neurons. (d) Example traces of a neuron producing a purely sustained response to low pH (left panel) that was also sensitive to the TRPV1 agonist capsaicin (right panel). (e) Example traces of a neuron producing a sustained response to low pH (left panel) that was insensitive to the TRPV1 agonist capsaicin (right panel). In (d) and (e), a wash period of at least 30 s was present between the two stimuli. Numbers in brackets refer to the number of neurons recorded from. \* $p < 0.05$ , \*\* $p < 0.01$  and \*\*\* $p < 0.001$ ; † $p < 0.05$  between articular and cutaneous neurons. TRPV1: transient receptor potential vanilloid 1.

significant difference between the amplitude of responses between articular and cutaneous neurons (Figure 5(h)).

## Discussion

In this study, we have characterized and compared the neurochemical and electrophysiological properties of identified articular and cutaneous sensory neurons in

the mouse. We find that cutaneous injection of retrograde tracer labels a higher percentage of lumbar DRG neurons than articular (ankle and knee) injection and that in both cases, the majority of neurons are peptidergic. Comparing the electrophysiological properties of articular and cutaneous neurons, we find that cutaneous neuron action potential HPD is longer than in articular neurons and that ASIC-like currents are of significantly

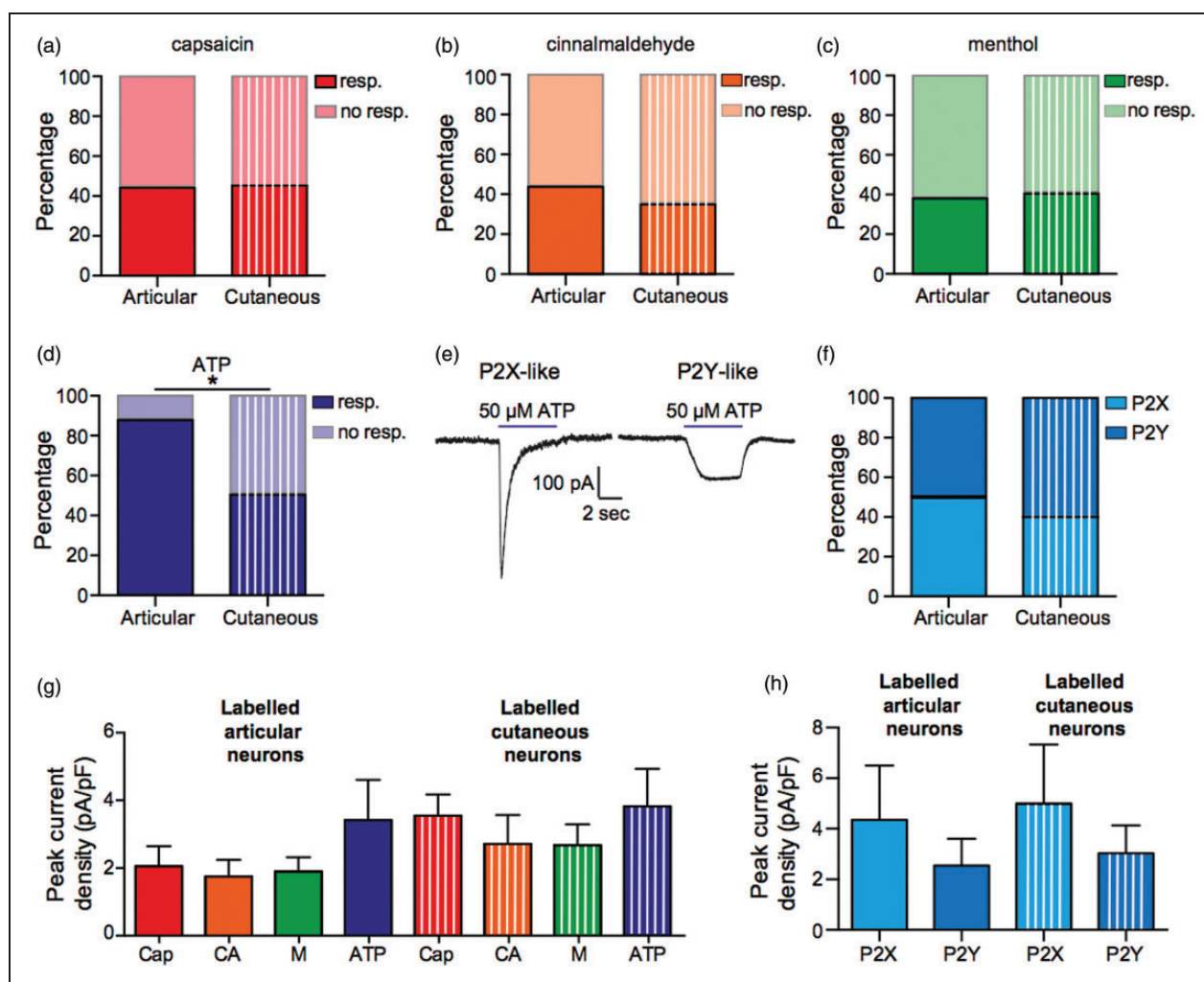


**Figure 5.** Chemosensitivity of articular and cutaneous neurons. (a–d) Percentage responders and nonresponders to capsaicin, cinnamaldehyde, menthol, and ATP; total number of neurons tested, articular  $n = 16$ , cutaneous  $n = 20$ . (e) Example of a P2X-like response (left panel) and a P2Y-like response (right panel) in response to ATP. (f) Percentage of ATP responses that were with P2X- or P2Y-like; total number of responses, articular  $n = 14$ , cutaneous  $n = 10$ . (g) Peak current responses to capsaicin (cap,  $1 \mu\text{M}$ ,  $n = 7$  and  $9$ ), cinnamaldehyde (CA,  $100 \mu\text{M}$ ,  $n = 7$  and  $7$ ), menthol (M,  $100 \mu\text{M}$ ,  $n = 6$  and  $8$ ) and ATP ( $50 \mu\text{M}$ ,  $n = 14$  and  $10$ ). (h) Peak current amplitudes of P2X- ( $n = 7$  and  $4$ ) and P2Y-like ( $n = 7$  and  $6$ ) responses to ATP. Resp. and no resp. refer to whether a neuron responded to the stimulus  $*p < 0.05$ .

greater amplitude in cutaneous neurons, whereas articular neurons respond more frequently to ATP than cutaneous neurons.

### Neurochemical properties of articular and cutaneous neurons

Although approximately the same volume of RetroBeads was injected into ankles/knees ( $\sim 2.5 \mu\text{l}/\sim 1.5 \mu\text{l}$ ) and subcutaneously into the plantar aspect ( $3 \times \sim 1 \mu\text{l}$ ) of each hind limb of mice in the articular and cutaneous groups, we observed that a significantly greater proportion of lumbar DRG neurons were labeled following cutaneous injection compared with articular injection (Figure 1). This finding is to be expected considering that the

number of neurons innervating cutaneous tissue in mammals is usually much greater than that which innervates the joints. For example, in the cat, afferent neurons in the posterior and medial articular nerves innervate the knee number 662 and 628, respectively,<sup>38</sup> whereas afferent neurons in the sural nerve innervate the lateral portion of the plantar hind paw, numbers 3596 afferent neurons.<sup>39</sup> However, it should be noted that subcutaneous injection could potentially label neurons innervating structures such as the periosteum, as well as neurons innervating the skin. Our finding that the L3 and L4 DRG contain the majority of labeled neurons following hind paw retrograde tracer injection replicates what others have identified.<sup>34</sup> Similarly, others have also found that the L3 and L4 DRG contain the majority



of labeled neurons following retrograde tracer injection into ankle or knee.<sup>24,40</sup>

With regard to the neurochemical phenotype of labeled neurons, both articular and cutaneous neurons contain a mixed population of myelinated (NF-200 positive) and unmyelinated neurons (peripherin positive), and the majority of labeled neurons are peptidergic (CGRP positive; Figure 2). In our immunohistochemistry analysis, we found that although the vast majority of articular neurons were peptidergic (79.38%), 5% were IB4-positive (Figure 2(e)) and thus likely nonpeptidergic fibers; in electrophysiology studies, we also observed a low proportion of IB4-positive articular neurons, 2/16 (12.5%). Previous studies have found either an absence of IB4 staining in knee joint afferents<sup>23,25</sup> or very low levels (1.5%) of staining,<sup>26</sup> whereas the majority of ankle afferents are CGRP positive.<sup>24</sup> Based upon previous literature, it is thus likely that the IB4-positive neurons we observed innervate the ankle, rather than the knee. For cutaneous neurons, we also noted a similar percentage of IB4-positive neurons using immunohistochemistry (26.01%) and electrophysiology (20%). Others have identified that neurons innervating the skin in various places of the body are IB4-positive at varying proportions<sup>27–29</sup> and indeed one other study that used a different retrograde tracer to that used in our study found that 19% of labeled plantar surface cutaneous afferents are IB4-positive.<sup>30</sup>

The general trend, although not significant, for decreased myelinated (NF-200 positive)/increased unmyelinated (peripherin positive) labeled neurons following cutaneous injection (Figure 2(e)) compared with articular injection (Figure 2(f)) may be the result of the higher ratio of unmyelinated C-fibers to A-fibers in those nerves innervating the skin<sup>41–45</sup> compared to the joints.<sup>38,39</sup> However, it should be noted that recent evidence shows that unmyelinated fibers do sometimes express NF-200 (~20%) and that large myelinated fibers in some cases express peripherin (~15%),<sup>35</sup> and, consequently, conclusions about fiber type based purely upon expression of either NF-200 or peripherin alone should be treated with caution. It is also possible that RetroBeads are preferentially endocytosed by unmyelinated neurons, which, as described earlier, are more prevalent in the skin than the joints. Although we have no evidence for biased labeling, it has been suggested that other neuronal tracers, such as wheat germ agglutinin and cholera toxin, are selectively taken up by different neuronal populations.<sup>46</sup> A second factor to consider is that neurons may dichotomize, such that cell bodies in the DRG project, axons that bifurcate and innervate multiple targets. For example, it has been shown that 1.6% of neurons innervating the rat hip joint also project to skin on the left medial portion of the knee.<sup>47</sup>

### *Electrophysiological properties of articular and cutaneous neurons*

No significant differences were observed with regard to the macroscopic voltage-gated inward currents recorded from articular and cutaneous neurons (Figure 3(c) and (d)). With regard to action potential parameters, the action potential HPD was significantly longer in cutaneous than articular neurons (Figure 3(h)), a possible explanation for the longer HPD would be enhanced expression of the voltage-gated sodium channel 1.8 (Nav1.8) because Nav1.8 is largely responsible for the inflection observed during the repolarization phase of action potentials.<sup>48</sup> We observed no significant difference in AHP duration between articular and cutaneous neurons (Figure 3(g)), but with regard to the values reported, it should be noted that a wide range of values have been published,<sup>49–51</sup> which reflects not only likely species differences but also the methodology used; here current injection lasted for 80 ms, which may influence the voltage-gated conductances that contribute to AHP duration.

During inflammation, such as that associated with rheumatoid arthritis, sensory neurons are exposed to a variety of stimuli that can both activate and sensitize them, such as prostaglandins, ATP, neuropeptides, and protons.<sup>52,53</sup> Here, we describe the basal characteristics of two different sensory neuron populations and determine their sensitivity to a variety of agonists for transduction channels: capsaicin (TRPV1), cinnamaldehyde (TRPA1), menthol (TRPM8), ATP (P2X/P2Y), and protons (e.g. ASICs and TRPV1). Tissue acidosis is a hallmark of inflammation and protons can induce depolarization via activation of ASICs, TRPV1, and certain G protein coupled receptors, as well as by inhibiting certain two-pore domain K<sup>+</sup> channels.<sup>54</sup> In both articular and cutaneous neurons, the majority of proton responses were ASIC-like, as determined by their inhibition by benzamil (64% and 72%, respectively Figure 4(a)–(c)). The percentage of transient ASIC-like currents in cutaneous neurons is slightly higher than what we have previously reported for a similar population of mouse cutaneous neurons<sup>36</sup> but is similar to what others have shown in the rat.<sup>17</sup> The amplitude of ASIC-like currents in cutaneous neurons was significantly larger than the amplitude of ASIC-like currents in articular neurons, which supports our previous observation, using a different retrograde tracer, that ASIC-like currents are of larger magnitude in cutaneous neurons compared with nonidentified neurons.<sup>36</sup> Our observation that all ASIC-like currents in cutaneous neurons were rapidly inactivating also supports our previous data<sup>36</sup> and that of others, which has shown that the rapidly inactivating ASIC3 subunit is the major contributor to hind paw skin neuron ASIC currents, with only a very



small percentage of neurons (4.7%) expressing the relatively slowly inactivating ASIC1a.<sup>17</sup> To our knowledge, this is the first description of ASIC-like currents in identified articular neurons, although immunohistochemistry has shown that ASIC3 is expressed by about 30% of sensory neurons that innervate the knee.<sup>55</sup> In both articular and cutaneous neurons, approximately half of the sustained responses to protons occurred in neurons that were also capsaicin sensitive, which indicates that although TRPV1 is responsible for many of the sustained currents observed that other conductances are also involved, an observation that others and ourselves have previously observed in different species.<sup>8,10,11,36,56</sup>

In both articular and cutaneous neurons, between 40 and 50% of neurons responded to agonists of TRPV1, TRPA1, and TRPM8 with there being no significant difference in the magnitude of responses. The reported sensitivity of DRG neurons to ligands of TRP channels varies depending upon the type of neurons analyzed and the culture conditions used. For example, TRPV1 sensitivity is reported from 16.5% in DRG dissociated from adult mice<sup>57</sup> to 83% in DRG dissociated from neonatal mice and cultured with nerve growth factor;<sup>58</sup> based upon functional analysis, TRPA1 and TRPM8 expression is reported as being approximately 30% and 20%, respectively.<sup>59–61</sup> Therefore, the sensitivity of both articular and cutaneous neurons to TRP channel agonists does not appear to be significantly enhanced or depressed compared with the general neuronal population as reported by others. The sensitivity of articular neurons to capsaicin was greater than the expression level detected by our immunohistochemistry data, i.e. only 20.83% TRPV1/RetroBead colocalization was observed using immunohistochemistry (Figure 2(e)), but electrophysiology found that 43.75% of neurons responded (Figure 5(a)); a similar, but smaller difference was observed for cutaneous neurons. This difference likely indicates the increased sensitivity of the electrophysiology technique, especially considering the small current amplitudes and indeed a similar disparity between immunohistochemistry and electrophysiology determination of TRPV1 expression has been previously noted.<sup>57</sup> Finally, whereas 87.5% of articular neurons responded to ATP, only 50% of cutaneous neurons responded, which suggests that articular neurons are more attuned to extracellular ATP levels. The finding that articular neurons are primed to sense ATP may indicate that fluctuation in articular ATP concentration is an initial step when damage to the joint occurs.

## Conclusions

This study is the first to combine immunohistochemical and functional comparative analysis of identified

articular and cutaneous neurons. Our findings demonstrate that cutaneous neurons have larger ASIC-like responses than articular neurons and that articular neurons respond more frequently to ATP.

## Acknowledgments

Thanks to Christoforos Tsantoulas for assistance with immunohistochemistry and members of the Smith lab for their technical assistance and help in preparing the manuscript.

## Author's contributions

ISS, ZH and JDB performed the experiments and analyzed the data. EStJS designed the experiments, performed the experiments, analyzed the data, and wrote the paper with ZH. All authors read and approved the final manuscript. ISS and ZH contributed equally.

## Declaration of Conflicting Interests

The author(s) declared no potential conflicts of interest with respect to the research, authorship, and/or publication of this article.

## Funding

The author(s) disclosed receipt of the following financial support for the research, authorship, and/or publication of this article: ZH and experiments were funded by an Arthritis Research Project Grant (Grant Reference 20930) and Early Career Research Grant from the International Association for the Study of Pain, both awarded to EStJS. ISS was funded by an Erasmus for Graduate Students grant from the University of Coimbra. JDB was funded by a Corpus Christi College Study and Travel Grant.

## References

1. Dubin AE and Patapoutian A. Nociceptors: the sensors of the pain pathway. *J Clin Invest* 2010; 120: 3760–3772.
2. Kavaliers M. Evolutionary and comparative aspects of nociception. *Brain Res Bull* 1988; 21: 923–931.
3. Lewin GR and Moshourab R. Mechanosensation and pain. *J Neurobiol* 2004; 61: 30–44.
4. Smith ES and Lewin GR. Nociceptors: a phylogenetic view. *J Comp Physiol A* 2009; 195: 1089–1106.
5. Sneddon LU. Evolution of nociception in vertebrates: comparative analysis of lower vertebrates. *Brain Res Rev* 2004; 46: 123–130.
6. Malin SA, Davis BM and Molliver DC. Production of dissociated sensory neuron cultures and considerations for their use in studying neuronal function and plasticity. *Nat Protoc* 2007; 2: 152–160.
7. Usoskin D, Furlan A, Islam S, et al. Unbiased classification of sensory neuron types by large-scale single-cell RNA sequencing. *Nat Neurosci* 2014; 18: 145–153.
8. Dirajlal S, Pauers LE and Stucky CL. Differential response properties of IB(4)-positive and -negative unmyelinated sensory neurons to protons and capsaicin. *J Neurophysiol* 2003; 89: 513–524.

9. Leffler A, Monter B and Koltzenburg M. The role of the capsaicin receptor TRPV1 and acid-sensing ion channels (ASICs) in proton sensitivity of subpopulations of primary nociceptive neurons in rats and mice. *Neurosci* 2006; 139: 699–709.
10. Liu M, Willmott NJ, Michael GJ, et al. Differential pH and capsaicin responses of *Griffonia simplicifolia* IB4 (IB4)-positive and IB4-negative small sensory neurons. *Neurosci* 2004; 127: 659–672.
11. Petruska JC, Napaporn J, Johnson RD, et al. Subclassified acutely dissociated cells of rat DRG: histochemistry and patterns of capsaicin-, proton-, and ATP-activated currents. *J Neurophysiol* 2000; 84: 2365–2379.
12. Stucky CL and Lewin GR. Isolectin B(4)-positive and -negative nociceptors are functionally distinct. *J Neurosci* 1999; 19: 6497–6505.
13. Molliver DC, Radeke MJ, Feinstein SC, et al. Presence or absence of TrkA protein distinguishes subsets of small sensory neurons with unique cytochemical characteristics and dorsal horn projections. *J Comp Neurol* 1995; 361: 404–416.
14. Lin YW, Min MY, Lin CC, et al. Identification and characterization of a subset of mouse sensory neurons that express acid-sensing ion channel 3. *Neuroscience* 2008; 151: 544–557.
15. Lechner SG, Markworth S, Poole K, et al. The molecular and cellular identity of peripheral osmoreceptors. *Neuron* 2011; 69: 332–344.
16. Sutherland SP, Benson CJ, Adelman JP, et al. Acid-sensing ion channel 3 matches the acid-gated current in cardiac ischemia-sensing neurons. *Proc Natl Acad Sci U S A* 2001; 98: 711–716.
17. Deval E, Noel J, Lay N, et al. ASIC3, a sensor of acidic and primary inflammatory pain. *EMBO J* 2008; 27: 3047–3055.
18. Rau KK, Petruska JC, Cooper BY, et al. Distinct subclassification of DRG neurons innervating the distal colon and glans penis/distal urethra based on the electrophysiological current signature. *J Neurophysiol* 2014; 112: 1392–1408.
19. Harriott AM and Gold MS. Electrophysiological properties of dural afferents in the absence and presence of inflammatory mediators. *J Neurophysiol* 2009; 101: 3126–3134.
20. Yan J, Wei X, Bischoff C, et al. pH-evoked dural afferent signaling is mediated by ASIC3 and is sensitized by mast cell mediators. *Headache* 2013; 53: 1250–1261.
21. Bielefeldt K, Ozaki N and Gebhart GF. Role of nerve growth factor in modulation of gastric afferent neurons in the rat. *Am J Physiol Gastrointest Liver Physiol* 2003; 284: G499–G507.
22. Molliver DC, Immke DC, Fierro L, et al. ASIC3, an acid-sensing ion channel, is expressed in metaboreceptive sensory neurons. *Mol Pain* 2005; 1: 35.
23. Aso K, Ikeuchi M, Izumi M, et al. Nociceptive phenotype of dorsal root ganglia neurons innervating the subchondral bone in rat knee joints: Characteristics of the subchondral bone afferents. *Eur J Pain* 2014; 18: 174–181.
24. Cho WG and Valtchanoff JG. Vanilloid receptor TRPV1-positive sensory afferents in the mouse ankle and knee joints. *Brain Res* 2008; 1219: 59–65.
25. Ivanavicius SP, Blake DR, Chessell IP, et al. Isolectin b4 binding neurons are not present in the rat knee joint. *Neuroscience* 2004; 128: 555–560.
26. Ferreira-Gomes J, Adães S, Sarkander J, et al. Phenotypic alterations of neurons that innervate osteoarthritic joints in rats: phenotype markers in neurons innervating OA knee joint. *Arthritis Rheum* 2010; 62: 3677–3685.
27. Ambalavanar R, Moritani M, Haines A, et al. Chemical phenotypes of muscle and cutaneous afferent neurons in the rat trigeminal ganglion. *J Comp Neurol* 2003; 460: 167–179.
28. Bennett DLH, Dmtrieva N, Priestley JV, et al. trkA, CGRP and IB4 expression in retrogradely labelled cutaneous and visceral primary sensory neurons in the rat. *Neurosci Lett* 1996; 206: 33–36.
29. Damann N, Rothermel M, Klupp BG, et al. Chemosensory properties of murine nasal and cutaneous trigeminal neurons identified by viral tracing. *BMC Neurosci* 2006; 7: 46.
30. Aoki Y, Ohtori S, Takahashi K, et al. Expression and co-expression of VR1, CGRP, and IB4-binding glycoprotein in dorsal root ganglion neurons in rats: differences between the disc afferents and the cutaneous afferents. *Spine* 2005; 30: 1496–1500.
31. Lu J, Zhou XF and Rush RA. Small primary sensory neurons innervating epidermis and viscera display differential phenotype in the adult rat. *Neurosci Res* 2001; 41: 355–363.
32. Lawson SN. Phenotype and function of somatic primary afferent nociceptive neurons with C-, Adelta- or Aalpha/beta-fibres. *Exp Physiol* 2002; 87: 239–244.
33. Katz LC, Burkhalter A and Dreyer WJ. Fluorescent latex microspheres as a retrograde neuronal marker for in vivo and in vitro studies of visual cortex. *Nature* 1984; 310: 498–500.
34. Rigaud M, Gemes G, Barabas M-E, et al. Species and strain differences in rodent sciatic nerve anatomy: implications for studies of neuropathic pain. *Pain* 2008; 136: 188–201.
35. Bae JY, Kim JH, Cho YS, et al. Quantitative analysis of afferents expressing substance P, calcitonin gene-related peptide, isolectin B4, neurofilament 200, and Peripherin in the sensory root of the rat trigeminal ganglion: neuronal marker expression in sensory root. *J Comp Neurol* 2015; 523: 126–138.
36. Smith ESJ, Omerbašić D, Lechner SG, et al. The molecular basis of acid insensitivity in the African naked mole-rat. *Science* 2011; 334: 1557–1560.
37. Waldmann R, Bassilana F, de Weille J, et al. Molecular cloning of a non-inactivating proton-gated Na<sup>+</sup> channel specific for sensory neurons. *J Biol Chem* 1997; 272: 20975–20978.
38. Langford LA and Schmidt RF. Afferent and efferent axons in the medial and posterior articular nerves of the cat. *Anat Rec* 1983; 206: 71–78.
39. Langford LA. Unmyelinated axon ratios in cat motor, cutaneous and articular nerves. *Neurosci Lett* 1983; 40: 19–22.
40. Salo PT and Theriault E. Number, distribution and neuropeptide content of rat knee joint afferents. *J Anat* 1997; 190(Pt 4): 515–522.

41. Illanes O, Henry J and Skerrett G. Light and electron microscopy studies of the ulnar, saphenous, and caudal cutaneous sural nerves of the dog. *Am J Anat* 1990; 187: 158–164.
42. Ochoa J and Mair WG. The normal sural nerve in man. I. Ultrastructure and numbers of fibres and cells. *Acta Neuropathol* 1969; 13: 197–216.
43. Scadding JW. The permanent anatomical effects of neonatal capsaicin on somatosensory nerves. *J Anat* 1980; 131(Pt 3): 471–482.
44. Schmalbruch H. Fiber composition of the rat sciatic nerve. *Anat Rec* 1986; 215: 71–81.
45. Smith ES, Purfürst B, Grigoryan T, et al. Specific paucity of unmyelinated C-fibers in cutaneous peripheral nerves of the African naked-mole rat: Comparative analysis using six species of Bathyergidae. *J Comp Neurol* 2012; 520: 2785–2803.
46. Valtschanoff JG, Weinberg RJ and Rustioni A. Peripheral injury and anterograde transport of wheat germ agglutinin-horse radish peroxidase to the spinal cord. *Neuroscience* 1992; 50: 685–696.
47. Miura Y, Ohtori S, Nakajima T, et al. Dorsal root ganglion neurons with dichotomizing axons projecting to the hip joint and the knee skin in rats: possible mechanism of referred knee pain in hip joint disease. *J Orthop Sci* 2011; 16: 799–804.
48. Blair NT and Bean BP. Roles of tetrodotoxin (TTX)-sensitive Na<sup>+</sup> current, TTX-resistant Na<sup>+</sup> current, and Ca<sup>2+</sup> current in the action potentials of nociceptive sensory neurons. *J Neurosci* 2002; 22: 10277–10290.
49. Djouhri L, Bleazard L and Lawson SN. Association of somatic action potential shape with sensory receptive properties in guinea-pig dorsal root ganglion neurons. *J Physiol* 1998; 513(Pt 3): 857–872.
50. Lawson SN, McCarthy PW and Prabhakar E. Electrophysiological properties of neurons with CGRP-like immunoreactivity in rat dorsal root ganglia. *J Comp Neurol* 1996; 365: 355–366.
51. Poole K, Herget R, Lapatsina L, et al. Tuning Piezo ion channels to detect molecular-scale movements relevant for fine touch. *Nat Commun* 2014; 5: 3520.
52. Basbaum AI, Bautista DM, Scherrer G, et al. Cellular and molecular mechanisms of pain. *Cell* 2009; 139: 267–284.
53. Gold MS and Gebhart GF. Nociceptor sensitization in pain pathogenesis. *Nat Med* 2010; 16: 1248–1257.
54. Holzer P. Acid-sensitive ion channels and receptors. *Handb Exp Pharmacol* 2009; 194: 283–332.
55. Ikeuchi M, Kolker SJ and Sluka KA. Acid-sensing ion channel 3 expression in mouse knee joint afferents and effects of carrageenan-induced arthritis. *J Pain* 2009; 10: 336–342.
56. Bevan S and Yeats J. Protons activate a cation conductance in a sub-population of rat dorsal root ganglion neurons. *J Physiol* 1991; 433: 145–161.
57. Caterina MJ, Leffler A, Malmberg AB, et al. Impaired nociception and pain sensation in mice lacking the capsaicin receptor. *Science* 2000; 288: 306–313.
58. Bonnington JK and McNaughton PA. Signalling pathways involved in the sensitisation of mouse nociceptive neurons by nerve growth factor. *J Physiol* 2003; 551(Pt 2): 433–446.
59. Bautista DM, Siemens J, Glazer JM, et al. The menthol receptor TRPM8 is the principal detector of environmental cold. *Nature* 2007; 448: 204–208.
60. Jordt SE, Bautista DM, Chuang HH, et al. Mustard oils and cannabinoids excite sensory nerve fibres through the TRP channel ANKTM1. *Nature* 2004; 427: 260–265.
61. Karashima Y, Talavera K, Everaerts W, et al. TRPA1 acts as a cold sensor in vitro and in vivo. *Proc Natl Acad Sci U S A* 2009; 106: 1273–1278.